Turk J Chem
31 (2007) , 531 – 550.
© TÜBİTAK
A REVIEW

Catalytic Processes for Clean Hydrogen Production from Hydrocarbons

Zeynep İlsen ÖNSAN
Department of Chemical Engineering, Boğaziçi University, Bebek 34342, İstanbul-TURKEY
e-mail: onsan@boun.edu.tr

Received 19.06.2007

Conversion of hydrocarbon fuels to hydrogen with a high degree of purity acceptable for fuel cell operation presents interesting challenges for the design of new selective catalysts and catalytic processes. Natural gas, LPG, gasoline, and diesel are regarded as promising hydrocarbon fuels. Methanol has received attention despite its toxicity, and ethanol has recently become of interest as a much less toxic and renewable resource. Selective catalytic processes considered for commercial use are based on steam reforming and partial oxidation of these fuels. Autothermal reforming (ATR) or indirect partial oxidation (IPOX) combines total oxidation (TOX), steam reforming (SR), and water-gas shift (WGS) reactions, where energy for the endothermic SR is supplied by exothermic TOX to provide an economically feasible process. Selective removal of CO from the hydrogen-rich reformate is achieved in high- and/or low-temperature WGS and preferential CO oxidation (PROX) reactors located between the reformer and the fuel cell. Recent works on catalytic hydrogen production and purification are surveyed, and research areas of future interest are underlined.

Key Words: Hydrogen production, hydrogen clean-up, SR, ATR, IPOX, WGS, PROX, fuel processors, engineered catalysts, micro-scale technologies.

Introduction

One of the novel approaches designed for meeting the strict standards set for air pollution control by reducing CO and NO_x emissions is the fuel cell technology. The proton exchange membrane fuel cell (PEMFC) powered by hydrogen shows potential for small-scale stationary applications in the short run and for mobile applications in the long run.[1,2] Since the infrastructure for hydrogen storage and distribution is presently lacking, on-board or in situ hydrogen production by processing fossil fuels with a distribution network is an attractive option. On-board generation of H_2 from gasoline to use as an alternative fuel for spark-ignition engines to extend the lean flammability of standard fuels includes thermal decomposition, steam reforming, partial oxidation, and exhaust gas reforming.[3] Hydrogen manufacture on medium to large scale for refinery usage and syngas applications involves steam reforming and focuses mostly on improved energy efficiencies and reduction in steam reformer sizes.[4] PEM fuel cells, on the other hand, require an almost pure supply of H_2, which calls for very selective processing that involves a combination of catalytic oxidation and steam reforming or direct partial oxidation.[5]

The focus of this review is the conversion of hydrocarbon fuels to H_2 with a degree of purity suitable for PEMFC operation, which presents challenges in the design of energy-efficient catalytic processes and highly selective solid catalysts. Processes considered for commercial use such as autothermal reforming (ATR) or indirect partial oxidation (IPOX) of fuels, which combines total oxidation (TOX), steam reforming (SR), and water-gas shift (WGS) reactions, and the selective removal of CO from hydrogen-rich reformate streams by high- and/or low-temperature WGS and preferential CO oxidation (PROX) are discussed within the framework of the generalized fuel processor system[6] shown in the Figure. Future trends in the development of integrated fuel processors including engineered catalysts and micro-scale technologies are also highlighted.

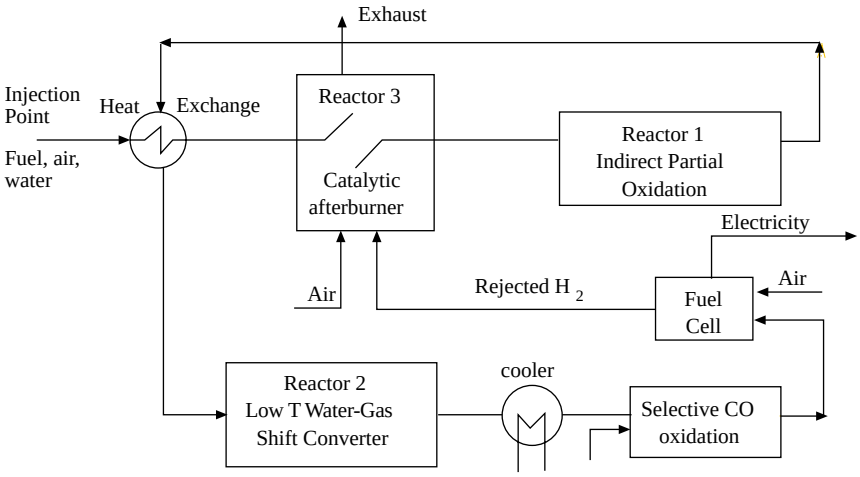

Figure. Schematic diagram of a generalized fuel processor-fuel cell system.[6]

Hydrocarbon Fuels

Hydrogen is both a key reactant and an energy carrier, and can be produced from various fuels among which existing fossil or petroleum-based fuels will continue to offer advantages for many years until the transition to renewable resources is completed. Natural gas, which is mainly methane, is one of the most attractive fuels for combined heat and power (CHP) applications; it accounts for almost half the feedstock used for H_2 production in the world and has the lowest greenhouse effect in terms of CO_2 emissions, in addition to high conversion efficiency and a wide transportation network.[7–9] LPG is also a promising fuel for similar reasons, because its delivery infrastructure is suitable for distributed power systems, and both of its components, propane and butane, have high conversion efficiencies.[10–14] Gasoline has an existing infrastructure and a high power density among available liquid fuels and is, therefore, an attractive alternative despite technical difficulties such as its content of aromatics, additives for improving antiknock properties, and sulfur.[5,15–19] Diesel has received attention owing to its importance in military applications and in auxiliary power units associated with fuel cells; nevertheless, problems related to coke formation on and sulfur poisoning of reforming catalysts await solution.[20,21] Multiple fuel processing is involved in the case of gasoline and diesel, since these fuels are not single compounds like methane and have several components, none of which outweighs others.

Among the oxygenated fuels that are hydrogen carriers, methanol has received considerable attention since its autothermal conversion can be initiated even at room temperature, and high efficiencies can be achieved under relatively mild conditions.[22–26] The feedstock used in the current industrial production of

methanol is syngas, obtained by steam reforming of natural gas; however, at present, methanol distribution through service stations is not possible, and substantial investment is required for its production, storage, and transportation because of its toxicity and volatility. Ethanol as a hydrogen source has the advantage of being producible by fermentation from renewable resources like agricultural wastes, it is much less toxic, and safer to handle and transport. Ethanol conversion and hydrogen production levels can change considerably with the type of catalyst and reaction conditions selected; consequently, process engineering aspects determine economic feasibility in ethanol SR.[27−30] Hydrogen production from bio-ethanol offers an attractive route with a nearly closed carbon loop since the carbon dioxide produced is consumed for biomass growth.[31]

Clean Hydrogen Production

The major chemical processes used for hydrogen production from hydrocarbon fuels for PEMFC applications are steam reforming, direct partial oxidation, and autothermal reforming:[5,32]

$$\text{SR: } C_nH_mO_p + steam \rightarrow \text{ carbon oxides + hydrogen} \qquad \Delta H_R > 0 \quad (1)$$

$$\text{POX: } C_nH_mO_p + air \rightarrow \text{ carbon oxides + hydrogen + nitrogen} \qquad \Delta H_R < 0 \quad (2)$$

$$\text{ATR: } C_nH_mO_p + steam + air \rightarrow \text{ carbon oxides + hydrogen + nitrogen} \qquad \Delta H_R \leq 0 \quad (3)$$

The hydrocarbon fuels proposed as possible hydrogen sources for PEMFC operation, chemical processes using these fuels for hydrogen production, thermodynamic characteristics of the basic reactions generating hydrogen, and theoretical energy requirements for producing hydrogen from different fuels were treated in detail.[32−36] Based on stoichiometric and thermodynamic considerations, it was shown that pure SR can produce a reformate stream containing ca. 70%-80% H_2 on a dry basis, whereas pure POX produces only ca. 35%-45% H_2.[33] Except for methanol SR, all processes generating hydrogen from hydrocarbons require sizeable water-gas shift converters for reducing the CO concentration and increasing the H_2 content of the reformate.[6]

Pure SR is highly endothermic, occurs at 1000-1150 K, requires external energy, and is unsuitable for operation under transient conditions. Direct partial oxidation (POX), on the other hand, is favored at high temperatures (1150-1900 K) and short residence times close to explosive limits; it produces H_2/CO ratios that are suitable for syngas applications.[5] An economical method of maximizing H_2 production is based on a combination of POX and high- and/or low-temperature WGS;[6,37] however, such hydrogen yields are still less than optimal for fuel cell systems. As a result, ATR or IPOX, which is a combination of SR and TOX, is the alternative preferred in most applications, because the energy for the endothermic SR reaction is supplied by the exothermic TOX reaction. Since fuel, water, and air are present in the feed, simultaneous high-temperature WGS reaction also occurs in the ATR reactor:

$$CO + H_2O \leftrightarrow CO_2 + H_2 \qquad \Delta H_R < 0 \quad (4)$$

The gas stream leaving the ATR reactor contains up to 8% CO on a dry basis, depending on the hydrocarbon fuel used;[38] hence, a 2-stage external WGS converter with high-temperature (573-723 K) and low-temperature (473-573 K) sections may be needed in the fuel processor to reduce the CO content first to 3%-4% and then to 0.5%-1%, respectively.[39] The temperature-equilibrium relationship dictates lower

temperatures in the second section for better CO removal. If the ATR effluent contains less than ca. 5% CO, a single low-temperature WGS reactor may be sufficient for achieving a maximum CO level of 2% in the exit stream.[6,36] Given that the Pt-based anode catalyst of the PEMFC at 353-373 K can tolerate only trace amounts of CO (< 10-50 ppm), a low-temperature preferential oxidation (PROX) reactor operating at 373-423 K is generally needed for final CO removal before the H_2-rich WGS effluent can be fed into the PEMFC:[5]

$$CO + {}^1\!/_2 O_2 \rightarrow CO_2 \qquad \Delta H_R < 0 \qquad (5)$$

Computer simulations based on both thermodynamic and kinetic approaches,[6,9,26,40] and comparing hydrogen production from different hydrocarbon fuels by IPOX or POX in a fuel processor with energy integration (Figure) have shown that (a) fuelling with both hydrocarbon and water is necessary; therefore, comparisons of the hydrogen yields of different fuels must be made not only in terms of theoretical yields {(moles of actual H_2 yield/moles of maximum theoretical H_2 yield) × 100} but also on weight-based yields {volume of H_2 fed into PEMFC at, e.g., 353 K/mass of (fuel + water) fed into fuel processor}, the latter yield being important especially for vehicular applications, and (b) the optimal water/fuel molar ratios for achieving maximum H_2 yields depend on the fuel, the conversion route (IPOX or POX) and the maximum bed temperature. Hydrogen yields obtained from computer simulations for methane (model for natural gas), propane (model for LPG), i-octane (model for gasoline) as well as for methanol and ethanol conversion by IPOX or POX and WGS are compared in Tables 1 and 2. Theoretical H_2 yields are given by Eq. (6) or Eqs. (7) and (4) for IPOX and POX of saturated hydrocarbons, respectively:

$$C_nH_{2n+2} + 2nH_2O \rightarrow nCO_2 + (3n+1)H_2 \qquad (6)$$

$$C_nH_{2n+2} + (n/2)O_2 \rightarrow nCO + (n+1)H_2 \qquad (7)$$

while those for IPOX and POX of alcohols are given by Eq. (8) or Eqs. (9) and (4), respectively:

$$C_nH_{2n+2}O + (2n-1)H_2O \rightarrow nCO_2 + 3nH_2 \qquad (8)$$

$$CH_3OH + (1/2)O_2 \rightarrow CO + H_2O + H_2 \qquad (9)$$

Steam Reforming (SR)

Steam reforming of hydrocarbons is highly endothermic and entails high reaction temperatures, typically >600 K for oxygenated and >1000 K for saturated hydrocarbons. Thermodynamic calculations reveal that the reforming of oxygenated hydrocarbons requires much less energy per mol of H_2 formed than do saturated hydrocarbons. Even then, the adiabatic temperature drops involved are rather large, e.g., for methanol SR, this is more than 400 K;[36] therefore, external energy has to be supplied for sustaining the SR of all fuels.

Table 1. Hydrogen yields obtained from computer simulations based on the kinetic approach.[6,9,26]

	Indirect Partial Oxidation					Direct Partial Oxidation				
Fuel	T_{max} (K)	Water/Fuel (mol/mol)	Yield 1	Yield 2	Yield 3	T_{max} (K)	Water/Fuel (mol/mol)	Yield 1	Yield 2	Yield 3
Methane	1100	3.45	202 (400)	50.5	500	1490	1.4	228 (300)	76	1060
Propane	1100	5.98	668 (1000)	66.8	850	1770	5.5	637 (700)	91	850
Octane	1100	11.41	1727 (2500)	69.1	1050	1840	14.4	1496 (1700)	88	770
Methanol	600	3.26	205.8 (300)	68.6	440	1370	0.2	57.4 (200)	28.7	318

Yield 1 = (mol H_2 produced/mol fuel fed) × 100; theoretical H_2 yields are shown in parentheses.
Yield 2 = (mol actual H_2 yield/mol theoretical H_2 yield) × 100;
Yield 3 = (volume of H_2 fed into PEMFC at 353 K/mass of fuel + water fed into the system) × 100; (mL/g).

Table 2. Hydrogen yields obtained from computer simulations for IPOX based on the thermodynamic approach.[26,38]

Fuel	T_{max} (K)	(mol/mol) S/C	Yield 1	Yield 2	Yield 3
Methanol	600	1.1	283 (300)	94.3	1160
Ethanol	1100	3.57	471 (600)	78.5	658
Propane	1100	2.0	770 (1000)	77.0	1275

Yield 1 = (mol H_2 produced/mol fuel fed) × 100; theoretical H_2 yields are shown in parentheses.
Yield 2 = (mol actual H_2 yield/mol theoretical H_2 yield) × 100;
Yield 3 = (volume of H_2 fed into PEMFC at 353 K/mass of fuel + water fed into the system) × 100; (mL/g).
S/C = Steam/Carbon = (mol H_2O fed + mol H_2O produced by TOX)/(n)(mol fuel fed – mol fuel consumed by TOX)

At high temperatures, catalyst deactivation by coke formation can be a problem; the choice of catalyst composition and addition of sufficient water into the feed stream are important for minimization of coking.[5] The equilibrium yields of Reaction (1) are strongly dependent on temperature, and the CO yield tends to increase with temperature. The reforming of oxygenated hydrocarbons (methanol and ethanol) produces mostly CO_2, some of which is later converted to CO via the rapid reverse WGS reaction that occurs in the reformer with hydrogen present.[36]

The SR of light hydrocarbons is a well-established industrial process and has been treated in the literature in considerable detail. Specific activities of metals supported on Al_2O_3 or MgO are reported to be Rh, Ru > Ni, Pd, Pt > Re > Co. Among those listed, nickel-based catalysts are widely used on a large scale because they are cost effective.[5,41−43] Since coke formation on Ni is higher than on Rh or Ru catalysts, the steam-to-carbon ratios (S:C) in the feed have to be adjusted to above stoichiometric for gasifying the coke formed at elevated temperatures; hence, these ratios may vary with the particular fuel used.[44] The (S:C) ratios that avoid coking were calculated approximately as being ≥ 2.5 for methane.[45,46] Support materials used for nickel catalysts can be modified to reduce coking; alkaline compounds such as Mg and K tend to help the gasification of coke, and CeO_2 improves catalytic activity while facilitating coke gasification through its high oxygen storage-release capacity.[47,48] Pd/CeO_2[49] and Pt-Ni/α-Al_2O_3[14] catalysts yield good results in alkane SR and hold promise for IPOX applications.

Steam reforming kinetics of alkanes over Ni-based catalysts shows a general trend of positive dependence on alkane concentration and a negative dependence on steam concentration.[42] Kinetics of methane SR and accompanying WGS reaction have been studied extensively, with some disagreement on the concentration dependencies.[50] The non-monotonic behavior of the system was quite well predicted by the Langmuir-Hinshelwood-Hougen-Watson (LHHW) rate expressions reported by Xu and Froment[51] for methane SR reactions towards CO and CO_2 as well as WGS over Ni-$MgAl_2O_4$ at 773-848 K. Other kinetic models proposed for methane SR over Ni-Al_2O_3 covered temperatures up to 1160 K and pressures up to 25 bars but did not take methane SR towards CO_2 into account.[52] Although LHHW kinetics is more informative about reaction mechanisms, power function rate expressions are frequently used for design and control purposes. The reaction orders and activation energies describing the SR kinetics of some alkanes [5,6,14,42,53−57] are summarized in Table 3.

Methanol SR has been studied using a variety of metal and metal-oxide based catalysts. The reaction is mildly endothermic; therefore, lower reaction temperatures between 473 and 673 K and low steam-to-carbon ratios produce high H_2 yield. Base metals, such as Ni, Co, Fe, Mn, Mo, and Cr, and some noble-metal based catalysts promote the production of syngas from methanol while Cu-based catalysts are selective for H_2 generation.[5] Pd-containing catalysts are also reported to have high methanol reforming activity and high H_2 production selectivity.[58] Power-function[59,60] and LHHW-type[23,24,60−62] rate expressions reported for methanol SR over Cu-ZnO/Al_2O_3 indicate that the dehydrogenation of methoxy groups formed on the surface is the rate-controlling step of the reaction mechanism. Simultaneous occurrence of the WGS reaction has also been considered.[23,24,61] The drawback of Cu catalysts is the sintering observed at temperatures above 600 K, which also restricts the relative H_2 generation efficiency of methanol in IPOX applications.[6,26] A deactivation model based on a comprehensive kinetic scheme and numerous rate measurements at high residence times was also developed for methanol SR over Cu-ZnO/Al_2O_3 catalysts.[63]

Table 3. Reaction orders and apparent activation energies of power function rate expressions reported for the steam reforming of some alkanes and alcohols (total pressure: 1 bar).

Fuel	Catalyst	T (K)	α (HC)	β (Steam)	γ (Hydrogen)	E_A (kJ/mol)	Reference
methane	Ni/MgO	723-823	1.0	–	–	110	42
methane	Ni/MgO	623-673	0.96	–0.17	0.25	60	5, 6, 54
methane	Ru/(α-Al_2O_3+MnO_x)	773-1173	< 1.0	–0.50	–	–	57
ethane	Ni/MgO	723-823	0.6	–0.4	0.2	76	5, 53
ethane	Ni/MgO	583-623	0.95	–0.46	0.38	80.6	5
propane	Ni/MgO	583-623	0.93	–0.53	0.86	45	5, 6
n-butane	Ni/SiO_2	673-723	0	1.0	–	–	5
n-butane	Pt-Ni/α-Al_2O_3	603-668	1.2	–0.18	–	80.7	14
n-heptane*	Ni/MgO	723-823	0.1-0.3	-0.2	0.8	67.8	55
i-octane	Ni-based/Al_2O_3	583-623	0.17	0.54	–	44 ± 2.2	56
methanol	CuO/ZnO/Al_2O_3	443-533	0.26	0.03	–0.20	–	59
methanol**	Cu-based (Zn, Zr, Ce, Fe, Cr)	493	0.5-0.6	0.02-0.05	– (0.2-0.3)	–	60
ethanol	Ru/γ-Al_2O_3	873-973	1	0	0	96	66
ethanol	Pt-Ni/α-Al_2O_3	673-723	1.25	–0.21	–	39.3 ± 2.1	67

*total pressure between 5 and 30 bars; **order in CO_2 also given as – (0.08-0.17).

The consideration of ethanol as a hydrogen source is new compared to methanol. Higher temperatures (600-1200 K) are required for the SR of ethanol because of its C-C bond. The current status of ethanol SR and the different catalysts used were recently reviewed,[27] and it was concluded that (a) ethanol conversions and hydrogen yields varied significantly with the type of catalyst, method of catalyst preparation, and reaction conditions, and (b) among the catalysts reported, Co/ZnO, ZnO, Rh/Al_2O_3, Rh/CeO_2, and Ni/La_2O_3-Al_2O_3 showed better performance. A more recent appraisal of catalytic ethanol SR provides insight into the effects of catalyst composition and process conditions on product distribution.[28] Hydrogen production by ethanol SR proceeds at atmospheric pressure, but calls for high temperatures and high water-to-ethanol ratios. Ni, Co, and Ni-Cu and noble metals such as Pt, Pd, and Rh over suitable supports are found promising, and the main difficulties are listed as byproduct formation and coke deposition. The nature and stability of surface species over Al_2O_3 or CeO_2-supported noble metal catalysts (Rh, Ru, Ir, Pd, and Pt) contacted with ethanol-water mixtures were studied by FTIR, TPD, and TPR methods to elucidate prevailing reaction mechanisms.[64] Ethylene, a product of ethanol dehydration, is formed mostly on Al_2O_3-supported noble metals, while a substantial quantity of acetaldehyde, a product of ethanol dehydrogenation, is also formed on CeO_2-supported catalysts. The deactivation pattern of Rh/CeO_2-ZrO_2 catalysts is consistent with carbon deposition, and total regeneration is possible at low temperatures.[65] Reports on intrinsic kinetic studies of ethanol SR are limited; Table 3 includes power-function rate expressions over Ru/Al_2O_3[66] and Pt-Ni/α-Al_2O_3[67] that show that ethanol conversion is directly proportional to ethanol partial pressure and is either independent of or mildly inhibited by steam partial pressure; these reaction orders agree with previous results on ethanol SR on Ni-based catalysts.[28,68] Ethanol SR over Co/Al_2O_3 at 673-973 K was recently described by LHHW type kinetic models that also accounted for WGS and ethanol decomposition reactions.[69]

Autothermal Reforming (ATR)

ATR is the most promising reforming technology for fuel cell systems, since the combination of catalytic TOX, SR, and high-temperature WGS reactions allows the design of more compact adiabatic reactors with low pressure drop.[70,71] Inlet temperature, steam-to-carbon, and oxygen-to-carbon ratios in the feed as well as reactor pressure are the independent variables of the ATR reactor, while the exit temperature and fuel conversion are the dependent variables. The parameter to be maximized is the H_2 yield (mol H_2 produced/mol fuel converted). Lower ATR reactor pressures are critical for maximizing H_2 yield. Higher steam-to-carbon ratios and reactor inlet temperatures favor H_2 production since less fuel has to be combusted for sustaining the reaction and hence lower oxygen-to-carbon ratios can be used;[72,73] higher steam-to-carbon ratios shift the coking boundary to a lower oxygen-to-carbon ratio and reduce coke formation.[74] The exit reformate contains H_2, CO, and CO_2, and relative concentrations are determined by the WGS reaction occurring in the ATR reactor if thermodynamic equilibrium is attained.[75] The optimal steam-to-carbon ratios for different fuels are reported as 4 for methane, 1.5 for methanol, 2.0 for ethanol, and 1.3 for surrogate gasoline.[36]

Catalyst development for the different steps involved in the production of PEMFC grade H_2 is a formidable task, and the trends in theoretical and experimental studies have recently been reviewed.[75−77] The successful ATR catalyst has to enable both TOX and simultaneous SR of the hydrocarbon fuel, operate at relatively low temperatures, and be resistant to both coke formation and poisoning by sulfur or halogen compounds likely to be present in the hydrocarbon. Fuel versatility, cost, durability, and operation under

transient conditions are also critical. Typical TOX (or POX) catalysts are oxide-supported Group VIII metals such as Rh, Pt, Pd, Ru, Ir, Co, and Ni.[78] The main catalyst component used in the ATR of gaseous alkanes (methane, ethane, propane, LPG, and butane) is Ni, promoted by precious metals like Pt, Pd, Rh, and Ru supported on solid solutions of ZrO_2 or Al_2O_3 with rare earth or alkaline earth oxides.[5,12,13,77,79] Transition metals supported on oxide-ion-conducting supports such as ceria, zirconia, or lanthanum gallate that have been doped with non-reducible elements such as Gd, Sm, or Zr have been patented for the reforming of higher hydrocarbons like i-octane.[75] The same study shows that the ATR of commercial-grade gasoline proceeds well at 1023 K over Pt supported on doped CeO_2, with the product gas containing 60% H_2 on a dry, diluent-free basis. Studies on the ATR of synthetic diesel fuel revealed that the impregnation of Ni or Pd in addition to Pt on Al_2O_3 or CeO_2-supported catalysts improves catalytic activity and sulfur resistance.[80−82] Catalyst characterization by TPR, TPD, and XPS indicated that the high catalyst stability was due to strong metal-metal and metal-support interactions rather than metal dispersion.[83]

The successful methanol SR catalyst CuO-ZnO/Al_2O_3 becomes inactive when exposed to oxygen unless the distribution of air in the reactor is not carefully controlled. Quaternary catalyst compositions such as CuO-ZnO/ZrO_2-Al_2O_3 have been designed to improve activity and stability in methanol ATR.[84−86] Methanol ATR over copper-based catalysts is also feasible if maximum temperatures can be kept at about 573 K. Methanol conversion is favored by high inlet temperatures and high steam-to-carbon ratios, whereas the undesirable CO selectivity is poorer at low feed temperatures. The promoting effect of ceria on copper oxide catalysts has been reported: the formation of a solid solution by the incorporation of Cu atoms into the CeO_2 lattice is responsible for the synergistic interaction.[87] The H_2 selectivity attained over Pd/ZnO catalysts in methanol ATR is reported to be nearly 80% at about 80% methanol conversion even in the absence of added water.[58] Pd/ZnO catalysts are stable at temperatures in excess of 600 K at which Cu-based catalysts sinter.[5] It was recently shown that the formation of a Pd-Zn alloy is critical for high selectivity for H_2 production.[88] Studies on the effect of adding Mg, Al, Zr, Ce, La, or Ru or a first-row transition metal to Pd/ZnO catalysts have shown that Cr, Fe, or Cu addition increases the selectivity to H_2 production by decreasing CO formation.[89]

Ni-based catalysts supported on Al_2O_3, MgO, La_2O_3, SiO_2, Y_2O_3, and YSZ with additions of Cu, Cr, Zn, Na, or K have been investigated for ethanol reforming reactions in the 523-873 K range.[30,90−92] It is generally accepted that Ni is responsible for the C-C bond cleavage, whereas additives like Cu or Cr promote methanol oxidation to produce H_2 and CO. Among the support materials tested, La_2O_3 and Y_2O_3 were found to be better than Al_2O_3. The catalytic performances of noble metal catalysts tested for ethanol ATR at 873-1123 K depended on the nature of the metallic phase (Rh, Pd, Ru, and Pt), the metal loading (0-5 wt%), and the nature of the support material (Al_2O_3, MgO, CeO_2, and TiO_2).[93] It was shown that Al_2O_3-supported catalysts promote ethanol dehydration to ethylene at lower temperatures, that ethylene is converted to H_2, CO, CO_2, and small amounts of CH_4 at higher temperatures, and that the order of activity for Al_2O_3-supported metals is Rh $\geq$ Ru $>$ Pd $>$ Pt = Ni.[77] Rh is significantly more active and more selective towards H_2 generation compared with Ru, Pt, and Pd.[93] On the other hand, with CeO_2/ZrO_2-supported catalysts, ethylene formation is not detected, and the order of activity of metals at higher temperatures is Pt $\geq$ Rh $>$ Pd. Incorporation of CeO_2 and/or La_2O_3 into Al_2O_3 supports has a promoter effect in the order CeO_2 $>$ CeO_2-La_2O_3 $>$ La_2O_3, suggesting a synergistic interaction between platinum and ceria that is diminished by the presence of lanthana.[94]

The kinetics of ATR is described by the simultaneous implementation of rate equations developed for TOX and SR of the hydrocarbon fuel considered as well as the rate equation for the WGS taking place concurrently in the ATR reactor. Simulation of methane ATR based on a one-dimensional heterogeneous fixed-bed reactor model[95] utilizes separate rate equations for methane TOX,[96] methane SR towards CO and towards CO_2 as well as the WGS[51] and carbon formation[97] reactions occurring simultaneously in the ATR reactor. Similarly, a one-dimensional reactor model developed for simulating methanol ATR[84] uses the kinetic model proposed by Peppley et al.[24] including the rate expressions for methanol SR towards CO_2 and H_2, for methanol decomposition to CO and H_2, and for the WGS reaction, while assuming that the total oxidation of methanol is instantaneous, i.e. limited by the oxygen supply. It has been shown that, once the light-off temperatures are reached, the total oxidation of hydrocarbons can be assumed to be very fast.[96] The first step in IPOX (or ATR) is the initiation of catalytic TOX, which is crucial in the heat management of the fuel processor system, and therefore the light-off temperatures of saturated and oxygenated hydrocarbons over different catalysts need to be known.[5,10,67,98]

Water-Gas Shift (WGS)

The exit product stream of the SR-based reformer contains up to 12% CO, while that of an ATR-based reformer contains 6%-8% CO.[70] Two stages of external WGS conversion are considered necessary for removing most of this CO by injecting steam while also producing additional H_2. WGS reaction is mildly exothermic ($\Delta H^\circ_{298} = -41$ kJ/mol), and its equilibrium constant decreases with increasing temperature; hence, the reaction is thermodynamically favored at temperatures where reaction kinetics is slow. Consecutive high-temperature (573-723 K) and low-temperature (473-573 K) WGS converters are therefore used to reduce the CO content first to 3%-4% and then to 0.5%-1%, respectively.[38,39,100] If the reformer effluent contains less than ca. 5% CO, a single low-temperature WGS reactor may be sufficient for attaining the maximum CO content of $\leq 2\%$ in the WGS exit.[6,36] The thermodynamics, kinetics, and industrial practice regarding WGS conversion have been reviewed in detail.[39,43,70,101]

Conventional high-temperature WGS catalysts based on Fe-Cr oxides are widely used in industrial processes owing to their low cost, long life, and acceptable sulfur tolerance. Cr_2O_3 is widely used as a stabilizer in industrial WGS catalysts; the precise mechanism by which the structural promotion of Fe_3O_4 by Cr^{3+} is achieved remains unresolved. Typical industrial catalysts contain about 8 wt% Cr_2O_3.[102] Iron oxide phases, FeO, Fe_2O_3, and Fe_3O_4, constitute the active phase and operate via an oxidation-reduction regenerative mechanism. Hence, careful control of temperature, H_2O/H_2 and CO_2/CO ratios is required for (a) supporting the interchange between different oxides of iron, which occurs above ca. 623 K, (b) circumventing the reduction of Fe oxides to Fe, which leads to methanation, and (c) avoiding condensation of water, which damages chromium oxides.[39,43] The low activity of Fe-Cr oxide catalysts calls for high reaction temperatures or large reactor volumes, both of which introduce problems. Therefore, possibilities for increasing the activity of Fe-Cr oxides were explored using base metal and noble metal promoters, among which Rh was found to be the most active promoter for Fe-Cr oxides and for Cr_2O_3.[102,103] These studies indicate that Cr_2O_3 can also catalyze the WGS reaction with suitable promoters such as Pt or Rh. However, there are environmental concerns related to Cr, and its substitution with less harmful components is desirable. Fe oxide catalysts doped with Al and Cu were tested and found to have activities similar to the commercial Fe-Cr-Cu catalyst.[104] Although the WGS reaction has been studied extensively, its mechanism

has not been fully elucidated. A comparison of regenerative (redox) and associative (formate formation) mechanisms confirms the predominance of the redox mechanism at higher temperatures.[103−105] The kinetics of high-temperature WGS reaction has been studied at length over the last few decades using LHHW and power-function rate expressions;[39,43,101,106] kinetic results agree with the redox mechanism.[107] Power law models are found adequate for most reactor design purposes. Table 4 includes some rate equations reported in the literature for high- and low-temperature WGS conversion.

Table 4. Reaction orders and apparent activation energies of power function rate expressions reported for high-temperature and low-temperature water-gas shift reaction.

Catalyst	T (K)	CO	H_2O	CO_2	H_2	E_A (kJ/mol)	Reference
Fe_3O_4-Cr_2O_3	600-723	0.90	0.25	−0.60	0.00	60	101
Fe_3O_4-Cr_2O_3	–	–	–	–	–	118	106
Rh-Fe_3O_4-Cr_2O_3	573-673	1.45	0.44	−0.12	−0.22	63	107
Cu-Zn	473-583	0.80	0.80	−0.90	−0.90	79	39
Cu-Ce(La)O_x	448-573	0.00	1.00	–	–	30.4	112
Ni-Ce(La)O_x	548-573	0.00	1.00	–	–	38.2	112
CuO-MnO_2	502	1.00	1.00	–	–	55	113
Pd-CeO_2	473-513	0.00	0.50	−1.00	−0.50	38	109
Rh, Pt or Pd-CeO_2	515	0.00	1.00	–	–	46±4	115

Rate = k $(CO)^a$ $(H_2O)^b$ $(CO_2)^c$ $(H_2)^d$ (1 - β); $\beta = (P_{CO2}P_{H2}/P_{CO}P_{H2O})\times$ (1/K); K = equilibrium constant for WGS.

The low-temperature WGS reaction is expected to reduce the CO content of reformate from 3%-4% to less than 1% and is catalyzed industrially by Cu-ZnO/Al_2O_3, which operates at 473-523 K.[38,39,70,100] Cu-ZnO/Al_2O_3 catalysts have been designed for a large-scale steady-state operation; they are not suitable for fuel cell power systems with duty cycles including frequent start-ups and shut-downs, because they require in situ reductive pretreatment with careful temperature control owing to the high exothermicity of the process; moreover, they are deactivated by steam condensation and poisoned by traces of sulfur and halides.[39,108] Exposure to air prompts an exothermic reaction of over 900 K, similar to rapid pretreatment in reducing gas, thus rendering Cu-ZnO catalysts unsafe for mobile use.[70] New regenerable Cu-Al_2O_3-$CuAl_2O_4$ catalysts with improved operational and safety features have been described.[109] Experimental evidence supports both regenerative and associative mechanisms for low temperature WGS over Cu-ZnO/Al_2O_3; either mechanism can proceed on the catalyst surface,[105] with the associative mechanism being more favored.[39] Efficiency of WGS catalysts is affected by the reversibility of Reaction 4, and reaction products strongly inhibit the forward rate. Kinetics of low temperature WGS over Cu-Zn in the presence of CO_2 and H_2 exhibit positive reaction orders close to unity in CO and H_2O, and negative reaction orders close to unity in CO_2 and H_2 as shown in Table 4.

CeO_2-supported transition metal catalysts were explored as alternatives to commercial Cu-ZnO/Al_2O_3 catalysts.[110,111] Cu-ceria had high activity, low cost, and better thermal stability than other Cu-based low temperature WGS catalysts, and La-doping of ceria further improved thermal stability.[111,112] Cu-ceria catalysts are as active as ceria-supported noble metals, but they are not sulfur resistant. Power law WGS kinetics over Cu and Ni catalysts supported on La-doped ceria was studied in the absence of product gases; the reaction orders and apparent activation energies of the forward rate are given in Table 4. A

redox mechanism involving the oxidation of CO adsorbed on the metal cluster by oxygen supplied to the metal interface from ceria by H_2O was suggested.[112] Another class of base metal WGS catalysts includes cobalt-containing catalysts like Co-Mn and Co-Cr that have higher activity than Fe-Cr above 573 K,[113] and Co-Mo catalysts with higher sulfur tolerance.[114] Lower activities of these catalysts at 473-573 K make them unsuitable for low temperature WGS converters. The commercial Cu-Zn-Al catalyst has much higher activity than all other low temperature WGS catalysts.[70]

The low temperature WGS reaction was also studied over CeO_2-supported noble metal catalysts. Water-gas shift kinetics over Pd, Pt, and Rh catalysts were roughly the same (Table 4), and the regenerative redox mechanism described for CeO_2-supported base metals was valid.[110,115] Diffuse reflectance and FTIR measurements on Pd-ceria indicated that ceria exists in a reduced state under WGS conditions.[110] Noble metal catalysts are thermally stable and not sensitive to contact with air or liquid water and, most significantly, they can easily be deposited on the walls of ceramic or metal alloy monolithic structures and are, therefore, more appropriate for the cyclic operation of fuel cell power systems; but they are expensive, and their performance under actual feed mixtures has yet to be confirmed. Table 4 indicates that most kinetic studies over CeO_2-supported noble or base metal catalysts were conducted at short run times in the absence of CO_2 and/or H_2. The ATR exit stream typically contains 45%-50% H_2 and 10% CO_2 besides CO, H_2O, and traces of unreacted hydrocarbons; the high temperature WGS converter produces additional CO_2 and H_2 during its CO removal.[39] Low activity and rapid first order deactivation were observed for low temperature WGS over Pt-ceria in such feed compositions.[116] There is no consensus on the causes of deactivation in the published literature.[116–118] The mechanisms proposed for WGS over Pt-ceria and Pd-ceria catalysts, their possible deactivation processes, and methods for enhancing catalytic activity by the use of promoters and improved pretreatment conditions were recently reviewed.[119] Pt catalysts supported on ZrO_2[120–122] and CeO_2-ZrO_2 [123,124] have received some attention for their sulfur tolerance despite their lower activity levels. The low temperature WGS performance of gold-based catalysts has been of current interest because of their activity and stability in the 473-623 K range and their non-pyrophoricity. Highly dispersed Au nano-particles (ca. 2 nm) were the key to the success of Au/Fe_2O_3,[125] Au/Fe_2O_3-ZrO_2,[126] and Au/TiO_2.[127] Ceria supports were also considered for gold catalysts,[128,129] and it was shown that Au trapped as an ion in oxide lattices resulted in a catalyst that was thermally stable, sintered less, and maintained its activity level.[130]

Preferential CO Oxidation (PROX)

The CO content in the low temperature WGS reactor output is determined by the reaction equilibrium constant at about 473 K and it corresponds to 0.5%-1.0% CO. It is necessary to remove this CO, as it poisons the Pt-based anode catalyst of the PEMFC. The most effective method of CO clean-up down to 10-50 ppm before the H_2-rich gases enter the PEM fuel cell is low temperature preferential oxidation (PROX) at 373-423 K, which has recently been reviewed at length.[5,39,70] The principal requirement here is to achieve almost 100% CO conversion with minimal H_2 oxidation.

The performance of PROX catalysts in actual reformate streams are affected by O_2/CO ratio, reactor temperature, and space velocity. Higher O_2/CO ratios favor CO and H_2 oxidation resulting in heat generation and temperature rise, both of which promote reverse water-gas shift (RWGS) and methanation reactions of CO and CO_2. Similarly, Pt-based catalysts produce CO by RWGS at low space velocities, due to extended

reaction times and depletion of the O_2 in the reactor.[70] Hence, successful PROX catalysts must be able to selectively and almost completely convert CO within a temperature bracket where the lower limit does not permit the condensation of the steam in the reformate and the upper limit does not promote RWGS and methanation.

Low temperature PROX catalysts generally contain a noble metal component, and Pt is well accepted in this respect. A comparison of reaction orders and activation energies reported in the literature for CO oxidation over unsupported Pt and Pt/γ-Al_2O_3 showed that orders in CO varied from -1.50 to 0, the O_2 order was close to unity, and the apparent activation energies ranged between 50 and 90 kJ/mol at T $\leq$ 500 K, whereas those determined at T $>$ 500 K were above 125 kJ/mol.[131]The structure sensitivity of CO oxidation over Pt/γ-Al_2O_3 was studied in the absence and presence of H_2 at various Pt dispersions, indicating that light-off temperatures and T_{50} (temperature for 50% conversion) of CO oxidation are lowered by the presence of H_2 in the feed,[132] but reaction kinetics and orders are not affected.[133,134] Similar behavior was observed for Ru/γ-Al_2O_3.[135] Reaction orders and apparent activation energies over some precious metal PROX catalysts are listed in Table 5.

Table 5. Reaction orders and apparent activation energies of power function rate expressions reported for low-temperature preferential CO oxidation.

Catalyst	T (K)	CO	O_2	E_A(kJ/mol)	Reference
Pt/γ-Al_2O_3	403-463	-(0.40-0.50)	0.95-1.15	96-120*	132
Pt/γ-Al_2O_3	423-523	-0.42 ± 0.05	0.82±0.05	71	133
Pt/γ-Al_2O_3	403-413	-0.51 ± 0.07	0.76±0.05	78±5	140
Pt/Al_2O_3	403-483	−0.47	0.66	62.7	149
Pt/mordenite	403-483	−0.69	0.68	40.1	149
Pt/CeO_2	329-345	−1.10	−0.20	62	131
Pt/CeO_2/γ-Al_2O_3	367-392	−1.30	0.10	42	131
Pt-Co/CeO_2/γ-Al_2O_3	383-403	−0.35	0.53	24.8	143
Pt-CeO_x/AC	383	−0.29	1.07	-	152
Pt-SnO_x/AC	383	0.96	−0.31	-	151
Ru/γ-Al_2O_3	408-473	−0.48	0.85	95±5	135
Au/α-Fe_2O_3	313-373	0.55±0.03	0.27±0.02	31	153

*443-493 K; increases with decreasing particle size

Pure noble metals on inert supports lack the selectivity required for PROX, and so promoters are added to facilitate CO oxidation via a dual-site mechanism with different adsorption sites for CO and oxygen. For example, the addition of CeO_2 to Pt/γ-Al_2O_3 decreased both the reaction order in O_2 and the apparent E_A for CO oxidation.[131] It was also found that Pt/CeO_2 performs better than Pt/γ-Al_2O_3 in terms of CO oxidation. The surface states and structural response of Pt/CeO_2 during PROX in the presence of H_2 were investigated using different spectroscopic techniques which indicated CO adsorbed on Pt particles and substantial water on the ceria surface.[136] It was proposed that oxygen-deficient ceria stabilizes the surface water, which represses H_2 oxidation and reacts at the metal-support interface with adsorbed CO in a WGS-type reaction to produce CO_2.[137] Both Pt/CeO_2 and Pd/CeO_2 are good CO oxidation catalysts, and while Pt/CeO_2 is an excellent PROX catalyst, Pd/CeO_2 is not active in the presence of H_2. The CO oxidation mechanisms on these 2 catalysts were studied by in situ experimental methods, which indicated that the PROX activity of Pd is hindered by its affinity for hydrogen chemisorption.[138] Platinum promoted by Co

or K appears to be the best PROX catalyst on oxide supports like Al_2O_3,[139,140] CeO_2-Al_2O_3,[141−143] CeO_2-MgO,[144] and MgO-Al_2O_3.[145] Recent reports on other Pt-based PROX catalysts include Pt/MnO_x-Al_2O_3,[146] Pt/SnO_2-Al_2O_3,[147] Pt/Fe_2O_3-Al_2O_3, [148] Pt/mordenite,[149] and activated carbon supported Pt-CeO_x and Pt-SnO_x.[150−152]

Interest in nano-gold catalysts has rapidly increased in recent years.[39,153] Although gold has long been classified as an extremely poor catalyst because of its inertness, remarkable CO oxidation activities have lately been reported in gas mixtures with or without H_2 for highly dispersed nano-gold particles/clusters with diameters less than 5 nm.[154−158] These studies confirm that CO oxidation activity is strongly related to particle size and to the nature of the metal-support interaction, both of which are critically dependent on the procedures used for catalyst preparation and pretreatment.[156,158−160] The PROX reaction studied over Au/MnO_x catalysts showed that higher CO oxidation selectivity was obtained at smaller Au particle sizes at T $\leq$ 353 K.[161] The addition of MnO_x and MgO to Al_2O_3-supported Au catalysts had similar effects at T $\leq$ 373 K, where MgO stabilized nano-gold particles whereas MnO_x acted as an oxygen source.[155−156] A comparative study of Au/MnO_x and Au/FeO_x catalysts in the 323-463 K range indicated a higher CO oxidation selectivity of 58% for Au/MnO_x at 403 K while 53% selectivity was achieved over Au/FeO_x at 323 K.[162] Kinetics of selective CO oxidation over Au/α-Fe_2O_3 at 313-373 K in H_2-rich gas[163] led to positive reaction orders for both CO and O_2 with a much lower activation energy compared to Pt-based catalysts (Table 5). Kinetic studies conducted at 273-353 K over several TiO_2, Co_2O_3, and Fe_2O_3-supported catalysts prepared by various techniques to give Au particle sizes of 3-33 nm showed that the reaction order in O_2 was ca. 0.40 while the order with respect to CO varied between 0.20 and 0.60; apparent activation energies reported for these catalysts ranged from 16 to 38 kJ/mol.[156]

Future Directions

The amount of hydrogen needed by a PEM fuel cell stack operating at about 40% efficiency is estimated as 37-41 mol H_2/h/kW.[33] Catalyst requirements of conventional fixed-bed SR, WGS, and PROX reactors in a methane processor feeding hydrogen to a 50 kW PEMFC unit were calculated to be approximately 11, 17, and 5 kg, respectively, based on appropriate intrinsic kinetic models.[164] For automotive applications, like passenger cars, 50 kW is the figure quoted. The total catalyst loading for the ATR, WGS, and PROX units of a methane processor feeding a 1.5 kW PEMFC is close to 1.5 kg,[165] while that of an integrated gasoline processor with a design scale of 1 kW is 1.2 L corresponding to about 1 kg of catalyst.[18] The amounts of catalyst and reactor volumes required affect the technical feasibility of fuel processors. The cost of precious metal catalysts as well as the need for careful temperature control and energy integration is forcing research towards the design of alternative catalysts and micro-structured reactors.[166]

The major challenges in catalyst research may be briefly listed as (a) reductions in the noble metal (mainly Pt) content of ATR catalysts and the design of alternative catalysts, e.g., perovskites, (b) new catalysts or improved designs for avoiding the reduction of robust Fe-oxides to metallic Fe in high temperature WGS, (c) catalyst alternatives with better thermal stability and pyrophoric properties as well as sulfur resistance for mobile and stationary applications in low temperature WGS converters, (d) cutbacks in the precious metal (mainly Pt) content of PROX catalysts by using apposite promoters and support materials, development of suitable gold-based catalysts, and exploration of base metals/metal oxides as substitute

catalysts for selective CO oxidation in H_2-rich streams containing both CO_2 and H_2O.

As yet, the design of efficient catalysts or processes is essential for the commercialization of fuel processors. The low values of the internal effectiveness factors of conventional ATR, WGS, or PROX catalysts packed in granular or pellet form has prompted the development of engineered catalysts using monolithic or foam substrates,[100,167,168] wall-coated catalysts,[169,170] and other micro-structured catalysts with new geometries,[171,172] which allow higher space velocities resulting in reduction of catalyst volumes and better heat transfer. Development of techniques for coating surfaces with various ATR, WGS, and PROX catalysts with durability for cyclic modes of operation presents challenges.[39,173] The major aim of the process intensification, or dynamic enhancement, is the thermal integration of the entire fuel processor system such that the energy requirement of the reactions can be supplied from the energy available at other units. Micro-scale technologies possess the attributes for process intensification and miniaturization and are expected to play a key role in the commercialization of efficient fuel processors.[166,174]

References

1. R. O'Hayre, S-W. Cha, W. Colella and F.B. Prinz, "**Fuel Cell Fundamentals**", Wiley, 2005.
2. F. Barbir, **"PEM Fuel Cells: Theory and Practice"**, Elsevier, 2005.
3. Y. Jamal and M.L. Wyszynski, **Int. J. Hydrogen Energy 19**, 557-72 (1994).
4. T. Rostrup-Nielsen, **Catal. Today 106**, 293-96 (2005).
5. D.L. Trimm and Z.İ. Önsan, **Cat. Rev.-Sci. Eng. 43**, 31-84 (2001).
6. A.K. Avcı, Z.İ. Önsan and D.L. Trimm, **Appl. Catal. A. Gen. 216**, 243-56 (2001).
7. J.N. Armor, **Appl. Catal. A. Gen. 176,** 159-76 (1999).
8. L. Ma and D.L. Trimm, **Appl. Catal. A. Gen. 138,** 265-73 (1996).
9. A.K. Avcı, D.L. Trimm and Z.İ. Önsan, **Chem. Eng. J. 90**, 77-87 (2002).
10. A.K. Avcı, D.L. Trimm, A.E. Aksoylu and Z.İ. Önsan, **Catal. Lett. 88**, 17-22 (2003).
11. Z.X. Liu, Z.O. Mao, J.M. Xu, N. Hess-Mohr and V.M. Schmidt, **Chinese J. Chem. Eng. 14**, 259-65 (2006).
12. B.S. Çağlayan, A.K. Avcı, Z.İ. Önsan and A.E. Aksoylu, **Appl. Catal. A. Gen. 280**, 181-88 (2005).
13. B.S. Çağlayan, Z.İ. Önsan and A.E. Aksoylu, **Catal. Lett. 102**, 63-7 (2005).
14. A.K. Avcı, D.L. Trimm, A.E. Aksoylu and Z.İ. Önsan, **Appl. Catal. A. Gen. 258,** 235-40 (2004).
15. L. Villegas, N. Guilhaume, H. Provendier, C. Daniel, F. Masset and C. Mirodatos, **Appl. Catal. A. Gen. 281**, 75-83 (2005).
16. D.L. Trimm, A.A. Adesina, Praharso and N.W. Cant, **Catal. Today 93**, 17-22 (2004).
17. A.A. Adesina, D.L. Trimm and N.W. Cant, **Chem. Eng. J. 99**, 131-6 (2004).
18. A. Qi, S. Wang, G. Fu and D. Wu, **J. Power Sources, 162**, 1254-64 (2006).
19. Q. Ming, T. Healey, L. Allen and P. Irving, **Catal. Today 77,** 51-64 (2002).
20. D.J. Liu, T.D. Kaun, H.K. Liao and S. Ahmed, **Int. J. Hydrogen Energy 29**, 1035-46 (2004).

21. J.C. Amphlett, R.F. Mann, B.A. Peppley, P.R. Roberge, A. Rodrigues and J.P. Salvador, **J. Power Sources 71**, 179-84 (1998).
22. L. Ma, C. Jiang, A. A. Adesina, D. L. Trimm and M. S. Wainwright, **Chem. Eng. J and Biochem. Eng. J. 62,** 103-11 (1996).
23. B.A. Peppley, J.C. Amphlett, L.M. Kearns and R.F. Mann, **Appl. Catal. A. Gen. 176,** 21-30 (1999).
24. B.A. Peppley, J.C. Amphlett, L.M. Kearns and R.F. Mann, **Appl. Catal. A. Gen. 176,** 31-49 (1999).
25. S.P. Asprey, B.W. Wojciechowski and B.A. Peppley, **Appl. Catal. A. Gen. 179,** 51-70 (1999).
26. A.K. Avcı, Z.İ. Önsan and D.L. Trimm, **Top. Catal. 22**, 359-67 (2003).
27. A. Haryanto, S. Fernando, N. Murali and S. Adhikari, **Energy and Fuels 19**, 2098-106 (2005).
28. P.D. Vaidya and A.E. Rodrigues, **Chem. Eng. J. 117**, 39-49 (2006).
29. V. Mas, R. Kiproes, N. Amadeo and M. Laborde, **Int. J. Hydrogen Energy 31**, 21-8 (2006).
30. J. Comas, F. Marino, M. Laborde and N. Amadeo, **Chem. Eng. J. 98**, 61-8 (2004).
31. F. Aupretre, C. Descorme and D. Duprez, **Catal. Commun. 3**, 263-7 (2002).
32. S. Ahmed and M. Krumpelt, **Int. J. Hydrogen Energy 26**, 291-301 (2001)
33. L. F. Brown, **Int. J. Hydrogen Energy, 26,** 381-97 (2001).
34. A.E. Lutz, R.W. Bradshaw, J.O. Keller and D.E. Witmer, **Int. J. Hydrogen Energy 28,** 159-67 (2003).
35. B.F. Hagh, **J. Power Sources 130**, 85-94 (2004).
36. T.A. Semelsberger, L.F. Brown, R.L. Borup and M.A. Inbody, **Int. J. Hydrogen Energy 29,** 1047-64 (2004).
37. P.S. Maiya, T.J. Anderson, R.L. Mieville, J.T. Dusek, J.J. Picciolo and U. Balachandran, **Appl. Catal. A. Gen. 196,** 65-72 (2000).
38. W. Ruettinger, O. Ilinich and R.J. Farrauto, **J. Power Sources 118**, 61-5 (2003).
39. D.L. Trimm, **Appl. Catal. A. Gen. 296,** 1-11 (2005).
40. E. Örücü, M. Karakaya, A.K. Avcı and Z.İ. Önsan, **J. Chem. Technol. Biotechnol. 80**, 1103-10 (2005).
41. J.R. Rostrup Nielsen, **"Catalytic Steam Reforming"**, Danish Technical Press, 1984.
42. J.R. Rostrup Nielsen, "**Catalytic Steam Reforming**" in Catalysis Science and Technology, J.R. Anderson and M. Boudart (Eds), vol. 5, p.1-117, Springer-Verlag, N. Y., 1984.
43. M.V. Twigg, Ed., **"Catalyst Handbook"**, Wolf Scientific Text, London, 1989.
44. D.L. Trimm, **Catal. Today 49**, 3-10 (1999).
45. J.R. Rostrup Nielsen, in **"Methane Conversion"**, D.M. Bibley et al. (Eds), Elsevier, Amsterdam, 1998.
46. T. Sperle, D. Chen, R. Lodeng and A. Holmen, **Appl. Catal. A. Gen. 282,** 195-204 (2005).
47. D.L. Trimm, **Catal. Today 37,** 233-8 (1997).
48. O. Sidjbat and D.L. Trimm, **Top. Catal. 11**, 279-82 (2000).
49. X. Wand and R.J. Gorte, **Appl. Catal. A. Gen. 224,** 209-18 (2002).
50. S.S.E.H. Elnashaie, A.M. Adris, A S. Al-Ubaid and M.A. Soliman, **Chem. Eng. Sci. 45**, 491-501 (1990).
51. J. Xu and G.F. Froment, **AIChE Journal 35**, 88-96 (1989).

52. T. Numaguchi and K. Kikuchi, **Chem. Eng. Sci. 43**, 2295-301 (1988).
53. M. Moayeri and D.L. Trimm, **J. Appl. Chem. Biotechnol. 26**, 419-24 (1976).
54. L. Ma, C.J. Jiang, A.A. Adesina and D.L. Trimm, Proc. 22^{nd} Australian and New Zealand Chemical Engineering Conference CHEMECA 94, vol.1, Perth, 1994.
55. P.B. Tottrup, **Appl. Catal. 4,** 377-89 (1982).
56. Praharso, A.A. Adesina, D.L. Trimm and N.W. Cant. **Chem. Eng. J. 99**, 131-6 (2004).
57. A. Berman, R.K. Karn and M. Epstein, **Appl. Catal. A. Gen. 282,** 73-83 (2005).
58. M.L. Cubeiro and J.L. Fierro, **J. Catal. 179**, 150-62 (1998).
59. C.J. Jiang, D.L. Trimm, M.S. Wainwright and N.W. Cant, **Appl. Catal. A. Gen. 93**, 245-55 (1993).
60. B. Frank, F.C. Jentoft, H. Soerijanto, J. Kröhnert, R. Schlögl and R. Schomacker, **J. Catal. 246**, 177-92 (2007).
61. C.J. Jiang, D.L. Trimm, M.S. Wainwright and N.W. Cant, **Appl. Catal. A. Gen. 97**, 145-58 (1993).
62. S. Patel and K.K. Pant, **J. Fuel Cell Sci. Technol. 3**, 369-74 (2006).
63. J.C. Amphlett, R.F. Mann, B.A. Peppley and C.P. Thurgood, **Stud. Surf. Sci. Catal. 139**, 205-12 (2001).
64. A. Erdohelyi, J. Rasko, T. Kecskes, M. Toth, M. Dömök and K. Baan, **Catal. Today 116**, 367-76 (2006).
65. H.-S. Roh, A. Platon, Y. Wang and D.L. King, **Catal. Lett. 110**, 1-6 (2006).
66. P.D. Vaidya and A.E. Rodrigues, **Ind. Eng. Chem. Res. 45**, 6618-8 (2006).
67. E. Örücü, F. Gökaliler, A.E. Aksoylu and Z.İ. Önsan, **Catal. Lett.** (2007) accepted for publication.
68. J. Sun, X-P. Qiu, F. Wu and W-T. Zhu, **Int. J. Hydrogen Energy 30**, 437-45 (2005).
69. D.R. Sahoo, S. Vajpai, S. Patel and K.K. Pant, **Chem. Eng. J. 125**, 139-47 (2007).
70. R. Farrauto, S. Hwang, L. Shore, W. Ruettinger, J. Lampert, T. Giroux, Y. Liu and O. Ilinich, **Annu. Rev. Mater. Res. 33**, 1-27 (2003).
71. J.K. Hochmuth, **Appl. Catal. B. Environ. 1**, 89-100 (1992).
72. B. Hagh, **Int. J. Hydrogen Energy 28**, 1369-77 (2003).
73. E. Doss, R. Kumar, R.K. Ahluwalia and M. Krumpelt, **J. Power Sources 102**, 1-15 (2001).
74. Y.-S. Seo, A. Shirley and S.T. Kolaczkowski, **J. Power Sources 108**, 213-25 (2002).
75. M. Krumpelt, T.R. Krause, J.D. Carter, K.P. Kopasz and S. Ahmed, **Catal. Today 77**, 3-16 (2002).
76. M. Andersen, O. Lytken, J. Engbaek, G. Nielsen, N. Schumacher, M. Johansson and I. Chorkendorff, **Catal. Today 100**, 191-7 (2005).
77. P.K. Cheekatamarla and J.M. Finnerty, **J. Power Sources 160**, 490-9 (2006).
78. K.H. Hofstad, J.H.B.J. Hoebink, A. Holmen and G.B. Marin, **Catal. Today 40**, 157-70 (1998).
79. B. Li, S. Kado, Y. Mukainakano, T. Miyazawa, T. Miyao, S. Naito, K. Okumura, K. Kunimori and K. Tomishige, **J. Catal. 245**, 144-55 (2007).
80. P.K. Cheekatamarla and A.M. Lane, **Int. J. Hydrogen Energy 30**, 1277-85 (2005).
81. P.K. Cheekatamarla and A.M. Lane, **J. Power Sources 152**, 256-63 (2005).

82. P.K. Cheekatamarla and A.M. Lane, **J. Power Sources 154**, 223-31 (2006).
83. P.K. Cheekatamarla and A.M. Lane, **J. Power Sources 153**, 157-64 (2006).
84. J.R. Lattner and M.P. Harold, **Catal. Today 120**, 78-89 (2007).
85. P.H. Matter, D.J. Braden and U.S. Ozkan, **J. Catal. 223**, 340-51 (2004).
86. P.H. Matter and U.S. Ozkan, **J. Catal. 234**, 463-75 (2005).
87. W.J. Shan, Z.C. Feng, Z.L. Li, Z. Jing, W.J. Shen and L. Can, **J. Catal. 228**, 206-17 (2004).
88. S. Liu, K. Takahashi and M. Aya, **Catal. Today 87**, 247-53 (2003).
89. S. Liu, K. Takahashi, K. Uematsu and M. Ayabe, **Appl. Catal. A. Gen. 277**, 265-77 (2004).
90. A.N. Fatsikostas, D.I. Kondarides and X.E. Verykios, **Catal. Today 75**, 145-55 (2002).
91. J. Sun, X.P. Qiu, F. Wu, W.T. Zhu, W.D. Wang and S.J. Hao, **Int. J. Hydrogen Energy 29**, 1075-81 (2004).
92. J. Sun, X.P. Qiu, F. Wu and W.T. Zhu, **Int. J. Hydrogen Energy 30**, 437-45 (2005).
93. M.A. Goula, S.K. Kontou and P.E. Tsiakaras, **Appl. Catal. B. Environ. 49**, 135-44 (2004).
94. E.C. Wanat, K. Wankataraman and L.D. Schmidt, **Appl. Catal. A. Gen. 276**, 155-62 (2004).
95. R.M. Navarro, M.C. Alvarez-Galvan, M. Cruz Sanchez-Sanchez, F. Rosa and J.L.G. Fierro, **Appl. Catal. B. Environ. 55**, 229-41 (2005).
96. A.K. Avcı, D.L. Trimm and Z.İ. Önsan, **Chem. Eng. Sci. 56**, 641-9 (2001).
97. L. Ma, D.L. Trimm and C. Jiang, **Appl. Catal. A. Gen. 138**, 275-83 (1996).
98. G.G. Kuvshinov, Y.I. Mogilnykh and D.G. Kuvshinov, **Catal. Today 42**, 357-60 (1998).
99. M.S. Wainwright and D.L. Trimm, **Catal. Today 23**, 29-42 (1995).
100. T. Giroux, S. Hwang, Y. Liu, W. Ruettinger and L. Shore, **Appl. Catal. B. Environ. 56**, 95-110 (2005).
101. D.S. Newsome, **Catal. Rev. Sci. Eng. 21**, 275-318 (1980).
102. C. Rhodes, B.P. Williams, F. King and G. Hutchings, **Catal. Commun. 3**, 381-4 (2002).
103. Y. Lei, N.W. Cant and D.L. Trimm, **Catal. Lett. 103**, 133-6 (2005).
104. S. Natesakhawat, X. Wang, L. Zhang and U.S. Ozkan, **J. Molec. Catal. A. Chem.** 260, 82-94 (2006).
105. C. Rhodes, G. Hutchings and A.M. Ward, **Catal. Today 23**, 43-58 (1995).
106. Y. Lei, N.W. Cant and D.L. Trimm, **Chem. Eng. J. 114**, 81-5 (2005).
107. R.L. Keiski, T. Salmi, P. Niemesto, J. Ainassaari and V.J. Pohjola, **Appl. Catal. A. Gen. 137**, 349-70 (1996).
108. A.A. Phatak, N. Koryabkina, S. Rai, J.L. Ratts, W. Ruettinger, R.J. Farrauto, G.E. Blau, W.N. Delgass and F.H. Ribeiro, **Catal. Today** (2007) doi: 10.1016/j.cattod. 2007.02.031
109. O. Ilinich, W. Ruettinger, X. Liu and R. Farrauto, **J. Catal. 247**, 112-8 (2007).
110. S. Hilaire, X. Wang, T. Luo, R.J. Gorte and J. Wagner, **Appl. Catal. A. Gen. 214**, 271-8 (2001).
111. T. Tabakova, V. Idakiev, J. Papavasiliou, G. Avgouropoulos and T. Ioannides, **Catal. Commun. 8**, 101-6 (2007).
112. Y. Li, Q. Fu and M. Flytzani-Stephanopoulos, **Appl. Catal. B. Environ. 27**, 279-91 (2000).
113. G.J. Hutchings, R.G. Copperthwaite, F.M. Gottschalk, R. Hunter, J. Mellor, S.W. Orchard and T. Sangiorgio, **J. Catal. 137**, 408-22 (1992).

114. R. Hakkarainen, T. Salmi and R.L. Keiski, **Appl. Catal. A. Gen. 99**, 195-215 (1993).
115. T. Bunluesin, R.J. Gorte and G.W. Graham, **Appl. Catal. B. Environ. 15**, 107-14 (1998).
116. J.M. Zalc, V. Sokolovskii and D.G. Löffler, **J. Catal. 206**, 169-71 (2002).
117. A. Goguet, F. Meunier, J.P. Breen, R. Burch, M.I. Petch and A.F. Ghenciu, **J. Catal. 226**, 382-92 (2004).
118. X. Wang, R.J. Gorte and J.P. Wagner, **J. Catal. 212**, 225-30 (2002).
119. R.J. Gorte and S. Zhao, **Catal. Today 104**, 18-24 (2005).
120. P.S. Querino, J.R.C. Bispo and M.D. Rangel, **Catal. Today 107-08**, 920-5 (2005).
121. H. Iida and A. Igarashi, **Appl. Catal. A. Gen. 303**, 48-55 (2006).
122. D. Tibiletti, F.C. Meunier, A. Goguet, D. Reid, R. Burch, M. Boaro, M. Vicario and A. Trovarelli, **J. Catal. 244**, 183-91 (2006).
123. D. Tibiletti, A. Amieiro-Fonseca, R. Burch, Y. Chen, J.M. Fischer, A. Goguet, C. Hardacre, P. Hu and A. Thompsett, **J. Phys. Chem. B. 109**, 22553-9 (2005).
124. S. Ricote, G. Jacobs, M. Milling, Y. Ji, P.M. Patterson and B.H. Davis, **Appl. Catal. A. Gen. 303**, 35-47 (2006).
125. D. Andreeva, T. Tabakova, V. Idakiev, P. Christov and R. Giovanoli, **Appl. Catal. A. Gen. 169**, 9-14 (1998).
126. J. Hua, Q. Zheng, K. Wei and X. Liu, **Catal. Lett. 102**, 99-108 (2005).
127. V. Idakiev, T. Tabakova, Z.–Y. Yuan and B.–L. Su, **Appl. Catal. A. Gen. 270**, 135-41 (2004).
128. Q. Fu, S. Kudriavtseva, H. Saltsburg and M. Flytzani-Stephanopoulos, **Chem. Eng. J. 93**, 41-53 (2003).
129. C.H. Kim and L.T. Thompson, **J. Catal. 244**, 248-50 (2006).
130. Q. Fu, W. Deng, H. Saltsburg and M. Flytzani-Stephanopoulos, **Appl. Catal. B. Environ. 56**, 57-68 (2005).
131. U. Oran and D. Üner, **Appl. Catal. B. Environ. 54**, 183-91 (2004).
132. B. Atalık and D. Üner, **J. Catal. 241**, 268-75 (2006).
133. M.J. Kahlich, H.A. Gasteiger and R.J. Behm, **J. Catal. 171,** 93-105 (1997).
134. M.M. Schubert, M.J. Kahlich, H.A. Gasteiger and R.J. Behm, **J. Power Sources 84**, 175-82 (1999).
135. Y.F. Han, M.J. Kahlich, M. Kinne and R.J. Behm, **Phys. Chem. Chem. Phys. 4**, 389-97 (2002).
136. O. Pozdnyakova, D. Teschner, A. Wootsch, J. Krohnert, B. Steinhauer, H. Sauer, L. Toth, F. C. Jentoft, A. Knop-Gericke, Z. Paal and R. Schlögl, **J. Catal. 237**, 1-16 (2006).
137. D. Teschner, A. Wootsch, O. Pozdnyakova, H. Sauer, A. Knop-Gericke and R. Schlögl, **Catal. Lett. 87**, 235-47 (2006).
138. O. Pozdnyakova, D. Teschner, A. Wootsch, J. Krohnert, B. Steinhauer, H. Sauer, L. Toth, F.C. Jentoft, A. Knop-Gericke, Z. Paal and R. Schlögl, **J. Catal. 237**, 17-28 (2006).
139. E.Y. Ko, E.D. Park, K.W. Seo, H.C. Lee, D. Lee and S. Kim, **Catal. Today 116**, 377-83 (2006).
140. D.H. Kim and M.S. Lin, **Appl. Catal. A. Gen. 224**, 27-38 (2002).
141. T. İnce, G. Uysal, A.N. Akın and R. Yıldırım, **Appl. Catal. A. Gen. 292**, 171-6 (2005).
142. J. Yan, J.X. Ma, P. Cao and P. Li, **Catal. Lett. 93**, 55-60 (2004).
143. G.N. Özyönüm, A.N. Akın and R. Yıldırım, **Turk. J. Chem.** 31, (2007).

144. G. Uysal, A.N. Akın, Z.İ. Önsan and R. Yıldırım, **Catal. Lett. 108**, 193-6 (2006).

145. S.H. Cho, J.S. Park, S.H. Choi and S.H. Kim, **J. Power Sources 156**, 914-20 (2006).

146. J.L. Ayastuy, M.P. Gonzales-Marcos, J.R. Gonzales-Velasco and M.A. Gutierrez-Ortiz, **Appl. Catal. B. Environ. 70**, 532-41 (2007).

147. G. Uysal, A.N. Akın, Z.İ. Önsan and R. Yıldırım, **Catal. Lett. 111**, 173-6 (2006).

148. X. Liu, O. Korotkikh and R.J. Farrauto, **Appl. Catal. A. Gen. 226**, 293-303 (2002).

149. S.H. Ren and X.L. Hong, **Fuel Processing Technol. 88,** 383-6 (2007).

150. Ş. Özkara and A.E. Aksoylu, **Appl. Catal. A. Gen. 251**, 75-83 (2002).

151. F.S. Baltacıoğlu, B. Gülyüz, A.E. Aksoylu and Z.İ. Önsan, **Turk. J. Chem. 31**, 455-464 (2007).

152. B. Gülyüz, **"Kinetics of Low Temperature CO Oxidation over Activated Carbon Supported Pt-CeO_x Catalysts"**, MS Thesis, Boğaziçi University, Istanbul, Turkey 2007.

153. G.C. Bond and D.T. Thompson, **Catal. Rev. Sci. Eng. 41**, 319-88 (1999)

154. S. Tsubota, T. Nakamura, K. Tanaka and M. Haruta, **Catal. Lett. 56**, 131-5 (1998).

155. R.J.H. Griesel and B.E. Nieuwenhuys, **J. Catal. 199**, 48-59 (2001).

156. T.V. Choudhary and D.W. Goodman, **Top. Catal. 21**, 25-34 (2002).

157. M.S. Chen and D.W. Goodman, **Science 306**, 252-5 (2004).

158. T.V. Choudhary and D.W. Goodman, **Appl. Catal. A. Gen. 291**, 32-6 (2005).

159. M. Bowker, A. Nuhu and J. Soares, **Catal. Today** (2007) doi: 10.1016/j.cattod.2007.01.201.

160. T.V. Choudhary, C. Sivadinarayana, C.C. Chusuei, A.K. Datye, J.P. Fackler Jr. and D.W. Goodman, **J. Catal. 207**, 247-55 (2002).

161. R.M.T. Sanchez, A. Ueda, K. Tanaka and M. Haruta, **J. Catal. 168**, 125-7 (1997).

162. A. Luengnaruemitchai, D.T.K. Thoa, S. Osuwan and E. Gulari, **Int. J. Hydrogen Energy 30**, 981-7 (2005).

163. M.J. Kahlich, H.A. Gasteiger and R.J. Behm, **J. Catal. 182,** 430-40 (1999).

164. J.M. Zalc and D.G. Löffler, **J. Power Sources 111**, 58-64 (2002).

165. Ö. Tan, **"Numerical Investigation of Hydrogen Production from Methane for Small Scale Stationary Fuel Cell Applications"**, MS Thesis, Boğaziçi University, Istanbul, Turkey, 2007.

166. A. Qi, B. Peppley and K. Karan, **Fuel Proc. Technol. 88**, 3-22 (2007).

167. A. Sirijaruphan, J.G. Goodwin Jr., R.W. Rice, D. Wei, K.R. Butcher, G.W. Roberts and J.J. Spivey, **Appl. Catal. A. Gen. 281**, 1-9 (2005).

168. A. Sirijaruphan, J.G. Goodwin Jr., R.W. Rice, D. Wei, K.R. Butcher, G.W. Roberts and J.J. Spivey, **Appl. Catal. A. Gen. 281**, 11-8 (2005).

169. C. Fukuhara, H. Ohkura, K. Gonohe and A. Igarashi, **Appl. Catal. A. Gen. 279**, 195-203 (2005).

170. C. Fukuhara, Y. Kamata and A. Igarashi, **Appl. Catal. A. Gen. 279**, 100-7 (2005).

171. C. Homy, L. Kiwi-Minsker and A. Renken, **Chem. Eng. J. 101**, 113- (2004).

172. V. Idakiev, Z.–Y. Yuan, T. Tabakova and B.–L. Su, **Appl. Catal. A. Gen. 281**, 149- 55 (2005).

173. S. Thybo, S. Jensen, J. Johansen, T. Johannessen, O. Hansen and U.J. Quaade, **J. Catal. 223**, 271-7 (2004).

174. J.-M. Commenge, L. Falk, J.-P. Corriou and M. Matlosz, **Chem. Eng. Technol. 28,** 446-58 (2005).